Reversible Oxidation of the Membrane Distal Domain of Receptor PTPα Is Mediated by a Cyclic Sulfenamide[†]

Jing Yang,[‡] Arnoud Groen,[§] Simone Lemeer,[§,||] Anne Jans,[§,||] Monique Slijper,[||] S. Mark Roe,[‡] Jeroen den Hertog,[§] and David Barford*,[‡]

Section of Structural Biology, Institute of Cancer Research, Chester Beatty Laboratories, 237 Fulham Road, London SW3 6JB, United Kingdom, Hubrecht Laboratory, Netherlands Institute for Developmental Biology, Uppsalalaan 8, 3584 CT Utrecht, The Netherlands, and Department of Biomolecular Mass Spectrometry, Bijvoet Center for Biomolecular Research, and Utrecht Institute for Pharmaceutical Sciences, Utrecht University, Sorbonnelaan 16, 3584 CA Utrecht, The Netherlands

ABSTRACT: Protein tyrosine phosphatases (PTPs) are fundamental to the regulation of cellular signalling cascades triggered by protein tyrosine kinases. Most receptor-like PTPs (RPTPs) comprise two tandem PTP domains, with only the membrane proximal domains (D1) having significant phosphatase activity; the membrane distal domains (D2) display little to no catalytic activity. Intriguingly, however, many RPTP D2s share the catalytically essential Cys and Arg residues of D1s. D2 of RPTPα may function as a redox sensor that mediates regulation of D1 via reactive oxygen species. Oxidation of Cys723 of RPTPα D2 (equivalent to PTP catalytic Cys residues) stabilizes RPTPα dimers, induces rotational coupling, and is required for inactivation of D1 phosphatase activity. Here, we investigated the structural consequences of RPTPα D2 oxidation. Exposure of RPTPα D2 to oxidants promotes formation of a cyclic sulfenamide species, a reversibly oxidized state of Cys723, accompanied by conformational changes of the D2 catalytic site. The cyclic sulfenamide is highly resistant to terminal oxidation to sulfinic and sulfonic acids. Conformational changes associated with RPTPα D2 oxidation have implications for RPTPα quaternary structure and allosteric regulation of D1 phosphatase activity.

The reversible tyrosine phosphorylation of proteins, reciprocally controlled by tyrosine kinases and phosphatases, is crucial to the regulation of diverse cellular processes, including growth, proliferation, and differentiation (*1*). Redox reactions, mediated by reactive oxygen species (ROS),[1] control PTP activity in response to a variety of hormones and growth factors (*2−6*). Generation of ROS accompanies PTK activation (*7, 8*), with oxidation-induced inhibition of PTP activity amplifying PTK-dependent signaling (*9−11*).

PTP-catalyzed protein dephosphorylation proceeds via a nucleophilic displacement reaction utilizing an essential cysteine residue conserved within the PTP signature motif Cys(X)$_5$Arg (*12−15*). The low pK_a of the catalytic cysteine necessary for its function (*16*) renders PTPs susceptible to inactivation by ROS-induced cysteine oxidation. However,

the reversibility of redox-mediated inactivation of PTPs requires that a reversibly oxidized state of the cysteine residue be stabilized at the PTP catalytic site and that formation of SO$_2$ and SO$_3$, two irreversibly oxidized species of cysteine, be suppressed (*17*). Crystallographic studies of the tyrosine specific cytosolic PTP1B revealed that the reversibly oxidized form of the enzyme was not the expected sulfenic acid or disulfide bond, but an oxidation state of cysteine termed a cyclic sulfenamide, a species not previously observed in proteins (*18, 19*). Generation of the cyclic sulfenamide inhibits catalytic activity by blocking the nucleophilic cysteine residue through a covalent bond of its thiol group with the neighboring main chain amide, a linkage that is accompanied by profound conformational transitions of the catalytic site PTP and pTyr loops. The oxidation properties of the catalytic Cys observed in PTP1B may be unique to the tyrosine specific subfamily of PTPs. Crystallographic and biochemical studies show that, in contrast to PTP1B, in the dual-specificity phosphatases KAP (*20*) and Cdc25 (*21−23*), lmPTPs (*24*), and lipid phosphatase PTEN (*25*), a disulfide bond linking the catalytic Cys residue to a proximal Cys is responsible for reversible oxidation and phosphatase inactivation. As in the cyclic sulfenamide of PTP1B, a disulfide bond suppresses overoxidation of the catalytic cysteine and is reversed by reductants. In another redox-regulatory mechanism, a stable and reversible sulfenic acid species was implicated as the oxidation-dependent inactive state of the dual-specificity phosphatase VHR (*17*).

* To whom correspondence should be addressed: E-mail: David. barford@icr.ac.uk. Telephone: +44 207 153 5420. Fax: +44 207 153 5457.

[‡] Institute of Cancer Research.

[§] Netherlands Institute for Developmental Biology.

[||] Utrecht University.

[1] Abbreviations: *p*NPP, *p*-nitrophenol phosphate; PTP, protein tyrosine phosphatase; RPTPα, receptor-like protein tyrosine phosphatase; RPTPα D1, receptor protein tyrosine phosphatase α (membrane proximal) domain 1; RPTPα D2, receptor protein tyrosine phosphatase α (membrane distal) domain 2; ROS, reactive oxygen species; SO$_2$, sulfinic acid; SO$_3$, solfonic acid; SN, cyclic sulfenamide.

The only precedent for a protein cyclic sulfenamide is the oxidized state of PTP1B, visualized directly by X-ray crystallography, and indirectly in solution by pulse—chase labeling and mass spectrometry experiments (*18*, *19*). Interestingly, examples of cyclic sulfenamides were reported some 30 years ago in studies of the synthesis of the antibiotic cephalosporin from penicillin precursors via the nucleophilic attack of a nitrogen atom on sulfenic acids (*26*–*28*). More recently, the synthesis of a cyclic sulfenamide species in vitro from a sulfenic acid precursor was demonstrated (*29*). There is now abundant evidence that numerous tyrosine specific PTPs are regulated via reversible and transient oxidation, suggesting that redox regulation of these PTPs may also feature a cyclic sulfenamide species (*5*, *6*). For example, in-gel phosphatase assays demonstrate that SHP-2 was reversibly oxidized in response to PDGF signaling (*30*), whereas ROS have been implicated in the suppression of both PTP1B and TCPTP activities in cells stimulated with insulin (*11*, *31*, *32*) and EGF (*7*).

While all cytosolic PTPs comprise a single catalytic domain linked to diverse regulatory or targeting domains, the majority of transmembrane receptor-like phosphatases comprise two PTP domains arranged in tandem (*1*, *33*). The membrane proximal D1 domain is responsible for all or most of the protein phosphatase activity with little to no phosphatase activity contributed by the D2 (distal) domain. Although essentially devoid of phosphatase activity, intriguingly most RPTP D2s share the conserved catalytic Cys and Arg residues of the PTP signature motif required for phosphatase activity. Furthermore, the crystal structures of LAR and RPTPα D2s indicated an environment of the PTP motif Cys residue essentially identical to that of catalytically active PTPs, which would be expected to promote a catalytic Cys with a reduced pK_a, enhancing its nucleophilicity (*34*, *35*). In striking experiments, the introduction of Tyr and Asp residues at the catalytic sites of LAR and RPTPα D2, residues required for pTyr recognition and general acid catalysis in PTP1B (*36*), conferred tyrosine specific phosphatase activity with catalytic rates equivalent to those of RPTP D1s and cytosolic PTPs (*34*, *37*, *38*). The catalytic Cys residues of RPTP D2s are therefore as reactive and oxidation sensitive as their counterparts in RPTP D1s (*39*).

A role for RPTPα D2 as a redox sensor was suggested from the findings that H_2O_2 induced numerous functional changes that were all dependent on the D2 catalytic Cys residue. Such changes include stabilization of RPTPα dimers, rotational coupling of the extracellular domain, and complete inactivation of D1 phosphatase activity (*39*, *40*). Development of a generic antibody that detects oxidation of the catalytic site Cys provided a direct observation of an oxidized PTP-motif Cys residue and revealed that D2 of RPTPα is more sensitive to oxidation than D1 (*41*, *42*). These results implicate a redox-dependent function of RPTP D2s, whereby the conserved Cys residue may function as a redox sensor, potentially mediating oxidation-dependent conformational changes of RPTPs and inside-out signaling (*40*).

Here, we investigate the structural consequences of RPTPα D2 oxidation by means of X-ray crystallography and explored the stability of the reversibly oxidized state in solution via catalytic activity measurements, mass spectrometry, and the oxidation specific antibody. We demonstrate that when RPTPα D2 crystals are exposed to oxidants (H_2O_2

and oxidized glutathione), oxidation of the conserved Cys residue generates a highly stable cyclic sulfenamide species, identical in chemical composition to PTP1B. These studies indicate that formation of the reversible cyclic sulfenamide is a general feature of the tyrosine specific PTPs and, importantly, provide a direct demonstration of the susceptibility of the D2 catalytic Cys to oxidation, with potential implications for redox-dependent regulation of RPTPα conformational changes and catalytic activity.

EXPERIMENTAL PROCEDURES

Structure Determination. Residues Ile512–Ser787 of murine RPTPα D2 were expressed from a pET-28a expression vector (a generous gift of Joseph Noel) and purified and crystallized under conditions similar to those described previously (*35*) except that prior to crystallization the protein was dialyzed into 10 mM Tris-HCl (pH 8.0), 100 mM NaCl, and 2 mM DTT. Crystals were prepared using the hanging drop vapor diffusion method at 14 °C by mixing protein at 12 mg/mL with an equal volume of a reservoir solution [13–15% (w/v) PEG 8K, 0.1 M sodium succinate (pH 5.5), 0.4 M LiSO₄, and 2 mM DTT]. Crystals belong to space group $C222_1$ with two molecules per asymmetric unit and the following cell parameters: $a = 74.7$ Å, $b = 94.7$ Å, and $c = 205.0$ Å. This crystal form differs from that reported by Sonnenburg et al. (*35*) (space group $P3_1$), although similar crystallization conditions, except for temperature, were used. Oxidation experiments were performed by incubating crystals in either 50 or 100 μM H_2O_2 or 10 mM oxidized glutathione for the specified times at 14 °C prior to crystal freezing (Table 1). For the reduction experiment, previously oxidized crystals were incubated in 10 mM DTT for 16 h. Data were collected at ESRF and processed using the CCP4 program suite (*43*). The initial structure in the series was determined by molecular replacement using the RPTPα D2 coordinates (*35*) (PDB entry 1P15) as a search model and refined using REFMAC, with subsequent structures being refined relative to this reference structure (Table 1).

Analysis of Oxidized PTPs Using the oxPTP Antibody. RPTPα D2 oxidation was assayed using an antibody, oxPTP, that specifically recognizes the sulfonic acid form of catalytic site cysteines of PTPs (*41*, *44*). Briefly, the GST–RPTPα D2 fusion protein, encoding residues 504–793, was bound to glutathione–agarose beads. All incubations and washes were performed in 20 mM Tris (pH 7.5). The proteins were reduced for 30 min in 10 mM dithiothreitol (DTT). Beads were washed twice and were incubated with 0.1 or 1.0 mM H_2O_2 for 0–24 h. Immediately after being treated, the proteins were processed for detection of (ir)reversibly oxidized catalytic cysteines by alkylation with 40 mM iodoacetic acid (IAA) for 30 min, reduction with 10 mM DTT for 30 min, and peroxidation with 0.1 mM pervanadate for 1 h (1 mM pervanadate and 1 mM Na₃VO₄ mixed with 5 mM H_2O_2, final concentrations, and left for at least 5 min at room temperature) to convert reduced cysteines irreversibly into the sulfonic acid form. Between treatments, the fusion proteins were extensively washed. Different orders of treatments were used to detect the reversibly oxidized catalytic cysteine [alkylation, reduction, and pervanadate (ARP)] or the sulfinic acid form [reduction, alkylation, and pervanadate (RAP)] as outlined in Figure 4B. After processing had been carried out, Laemmli sample buffer was added, and the

Table 1: Crystallographic Data Collection and Refinement Statistics[a]

	50 μM H₂O₂ for 30 min	50 μM H₂O₂ for 1.5 h	50 μM H₂O₂ for 3 h	100 μM H₂O₂ for 6 h	50 μM H₂O₂ for 16 h	10 mM GSSG for 12 days	reduced DTT	DTT for 0 h, control	DTT for 16 h, control
space group	$C222_1$	$C222_1$	$C222_1$	$C222_1$	$C222_1$	$C222_1$	$C222_1$	$C222_1$	$C222_1$
cell parameters (Å)	$a = 74.82$, $b = 94.79$, $c = 205.80$	$a = 75.29$, $b = 95.94$, $c = 205.84$	$a = 74.90$, $b = 94.66$, $c = 205.71$	$a = 75.0$, $b = 94.68$, $c = 205.62$	$a = 74.65$, $b = 94.79$, $c = 204.82$	$a = 75.19$, $b = 94.62$, $c = 207.39$	$a = 71.79$, $b = 97.31$, $c = 198.39$	$a = 74.63$, $b = 95.36$, $c = 204.86$	$a = 74.47$, $b = 95.39$, $c = 204.66$
beamline	ID14.2	ID23.1	ID14.4	ID14.4	ID14.4	ID14.4	ID14.4	ID14.3	ID14.2
resolution (Å)	2.3	2.1	1.90	2.0	1.85	2.5	2.4	2.4	2.3
R_{merge}	0.065 (0.262)	0.082 (0.324)	0.063 (0.328)	0.055 (0.141)	0.048 (0.387)	0.076 (0.12)	0.082 (0.136)	0.109 (0.323)	0.066 (0.306)
$I/\sigma I$	7.0 (2.5)	4.8 (1.2)	6.5 (1.5)	8.4 (4.5)	9.1 (1.9)	6.1 (5.5)	5.0 (4.2)	2.4 (1.0)	5.3 (1.7)
completeness (%)	99.2 (99.2)	99.4 (99.2)	95.3 (77.6)	80.3 (49.5)	74.3 (40.6)	94.2 (81.1)	94.1 (81.0)	99.9 (99.9)	99.2 (99.2)
multiplicity	3.7 (3.5)	4.0 (4.1)	3.7 (2.3)	3.1 (2.1)	4.0 (2.1)	5.0 (3.5)	4.0 (2.8)	4.0 (4.0)	4.0 (3.7)
no. of reflections	119994	176131	202962	122748	219282	128785	102476	115543	130217
detector	ADSC	ADSC	ADSC	ADSC	ADSC	ADSC	ADSC	MAR	ADSC
R-factor	0.226	0.230	0.217	0.208	0.212	0.212	0.232	0.241	0.247
R_{free}	0.290	0.278	0.249	0.241	0.245	0.243	0.301	0.325	0.296
Cys723 MolA	60% SN[b]	SN[b]	SN[b]	SN[b]	SN[b]	SN[b]	SH[c]	SH[c]	SH[c]
Cys723 MolB	90% SH[c]	SN[b]	SN[b]	SN[b]	SO₂[d]	SO₃[e]	SH[c]	SH[c]	SH[c]

[a] Figures in parentheses refer to the highest-resolution shell. [b] Cyclic sulfenamide. [c] Free thiol. [d] Sulfinic acid. [e] Sulfonic acid.

samples were boiled for 5 min and run on a 10% SDS–polyacrylamide gel (5 μg of protein per lane). Samples were transferred to PVDF membrane by semidry blotting. For detection with the oxPTP antibody, the blots were blocked in 0.1% BSA, 0.1% Tween in 50 mM Tris (pH 7.5), and 150 mM NaCl for 1 h or overnight and incubated with the oxPTP antibody (1.5 h at room temperature or overnight at 4 °C). Subsequently, a HRP-coupled goat anti-rabbit antibody (1:10000, BD Pharmigen) was used, and the antibody signals were visualized by enhanced chemiluminescence (ECL). The membranes were stripped and reprobed with the anti-RPTPα antibody (*45*) to monitor equal loading of the fusion protein.

MALDI-ToF Mass Spectrometry. All reactions and washing steps were performed in 20 mM Tris-HCl (pH 7.5). GST fusion proteins of RPTPα D2 were immobilized on gluthatione–Sepharose beads and incubated with 10 mM DTT. Beads were washed and incubated with 0.1 mM H₂O₂ for 0.5–24 h at room temperature. Subsequently, beads were treated with 100 mM iodoacetamide for 30 min at room temperature, to derivatize the unaffected cysteines. Finally, beads were washed and incubated with 10 mM DTT for 10 min to reduce singly oxidized cysteines. The fusion protein was subjected to overnight tryptic digestion. For desalting, peptides were adsorbed on C₁₈ ZipTips (Millipore) and washed with 0.1% trifluoroacetic acid (TFA). Peptides retained on the columns were eluted using α-cyano-4-hydroxycinnamic acid (10 mg/mL) in 10% acetonitrile and 0.1% TFA. Peptide mass fingerprint spectra were recorded using matrix-assisted laser desorption ionization mass spectrometry (MALDI-ToF/ToF; AB 4700 proteomics analyzer, Applied Biosystems, Framingham, MA). This instrument is equipped with a 200 Hz Nd:YAG laser operating at 355 nm. Experiments were performed in a reflectron positive ion mode using delayed extraction. Typically, a total of 7500 shots were acquired per spectrum, and the signal was averaged. MALDI-ToF/ToF spectra were analyzed using the Applied Biosystems Data Explorer software.

Catalytic Activity Measurements. The catalytic activity of RPTPα D2 was measured using 50 mM *p*-nitrophenol phosphate (*p*-NPP) as a substrate in a reaction buffer of 50 mM MES (pH 6.5), 100 mM NaCl, 0.5 mM EDTA, and RPTPα D2 (Ile512–Ser787) at a concentration of 300 μg/mL. To determine the reversibility of the oxidation reaction, the activity of the RPTPα was measured (i) prior to exposure

to H₂O₂, (ii) following an 18 h incubation with 50 μM H₂O₂ at 14 °C, and (iii) after a 3 h incubation of the oxidized protein with 25 mM DTT at 20 °C. Hydrolysis of *p*-NPP was monitored at 410 nm, and protein concentrations were determined, after removal of the aggregated protein by high-speed centrifugation, at the three time points to estimate specific activity.

Quantitative Gel Filtration. Reduced and oxidized RPTPα D2 (Ile512–Ser787) were loaded onto an analytical gel filtration column (Superdex 200 HR10/30, GE Healthcare) at 3 mg/mL in a buffer comprising 50 mM Tris-HCl (pH 8.0) and 100 mM NaCl. The oxidized protein was prepared by dialysis against 100 μM H₂O₂ for 16 h. Oxidation of the protein was confirmed by measuring its catalytic activity. The apparent molecular weight of the protein was estimated by calibrating the gel filtration column using molecular weight standards.

RESULTS

Structure of RPTPα D2. Crystallization of RPTPα D2 at 14 °C in our study yielded an orthorhombic crystal form ($C222_1$) differing from the trigonal crystals ($P3_1$) obtained at 4 °C by Sonnenburg et al. (*35*). The two molecules of RPTPα D2 in the $C222_1$ asymmetric unit associate to form a dimer identical to the RPTPα D2 dimers of the $P3_1$ crystals (*35*). The dimer interface is created from a surface of the molecule opposing the catalytic site. Both crystallographic independent subunits of RPTPα D2 (designated MolA and MolB) adopt essentially identical conformations (rmsd of 0.6 Å for equivalent Cα atoms). In our structure, residues 523–532 at the N-terminus of the D2 domain assume an α-helical conformation (equivalent to α2′ of PTP1B) (*46*) (Figure 1A), in contrast to their disordered state in the structure of Sonnenburg et al. (*35*). Significantly, an equivalent α-helix is present in all other cytosolic PTPs [PTP1B (*46*) and SHP-2 (*47*)] and receptor PTP structures [D1 of RPTPα and RPTPμ (*48*, *49*) and D1 and D2 of LAR and CD45 (*34*, *50*)]. In these PTP structures, α2′ is preceded by helix α1′, defining the N-terminus of the tyrosine specific PTP domain (*46*). Multiple-sequence alignment of RPTPs (refs *33* and *34* and data not shown) predicts an equivalent α1′ of RPTPα D2 comprising residues 502–514. These residues were not included in the RPTPα D2 domain we crystallized.
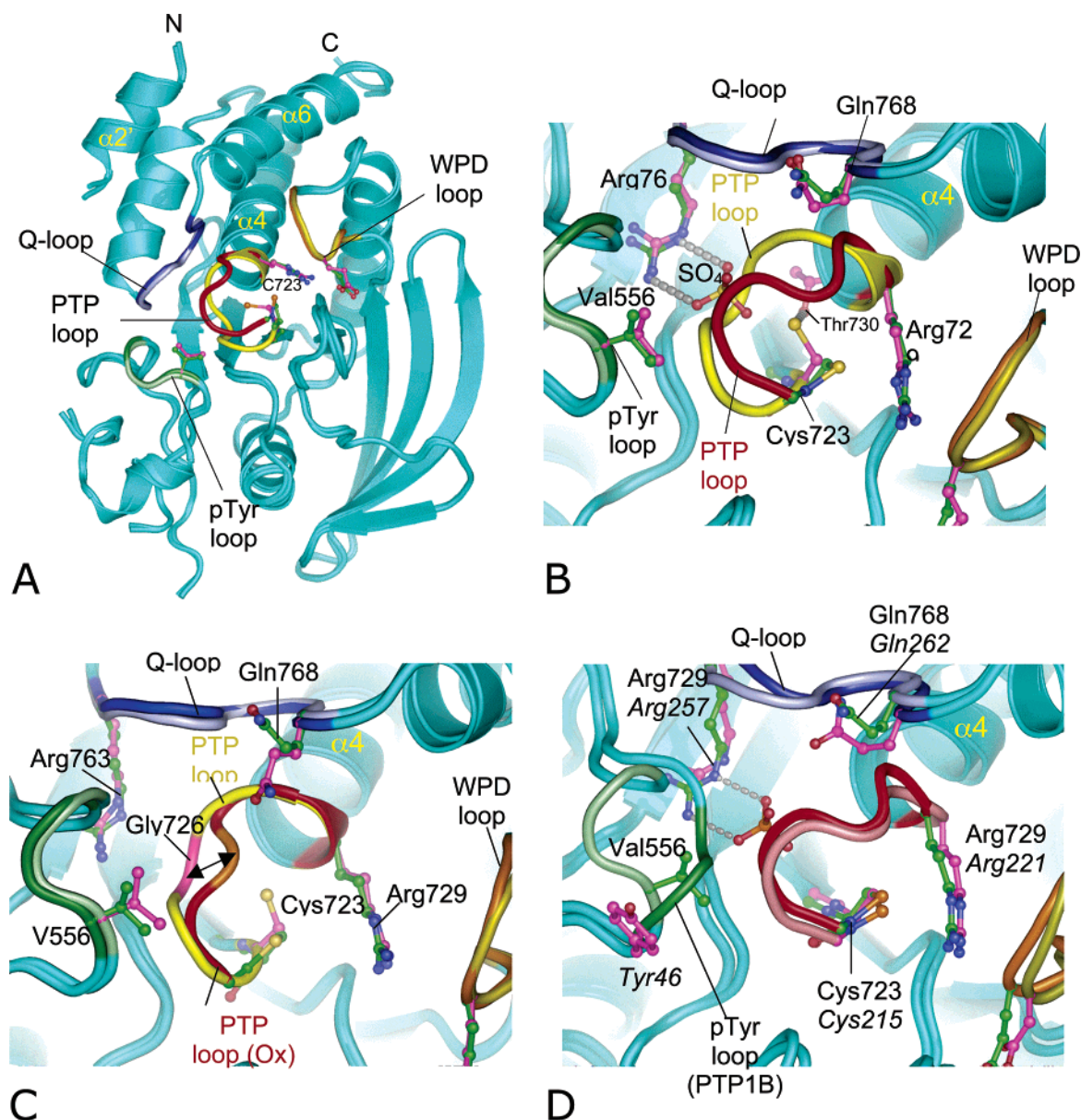
FIGURE 1: Oxidation-induced structural changes of RPTPα D2. (A) Overall view of RPTPα D2 MolA. Conformational changes are restricted to the PTP loop. Side chain carbon atoms are colored purple and green for reduced and oxidized states, respectively. Details of conformational changes of the PTP loop in MolA (B) and MolB (C). SO₄ represents sulfate. The change in the position of Gly726 in the PTP loop is denoted with an arrow in panel C. (D) The oxidized conformation of the PTP loop of RPTPα D2 MolA is identical to oxidized PTP1B (PTP1B side chains colored purple and residue numbers in italics). This figure was created using PYMOL.

Overall, the structure of RPTPα D2 resembles that of other tyrosine specific PTPs (Figure 1A). The domain is composed of a large central β-sheet flanked on both side by α-helices. Residues of the PTP signature motif (Cys-Xaa₅-Arg-Ser/Thr, residues 723−730) connect the central β-strand with the N-terminus of helix α4, creating a cradlelike structure, located at the center of the molecule, ideally configured for engaging a terminal phosphate group of a phosphorylated substrate. The side chain of the conserved Cys residue of the PTP motif (Cys723) projects into the PTP loop cradle and accepts a hydrogen bond from the side chain of Thr730 (Figure 1B).

Oxidation of RPTPα D2 Generates a Cyclic Sulfenamide Species. We performed a total of six oxidation experiments with RPTPα D2 crystals. Crystals were exposed to either 50 or 100 μM hydrogen peroxide over a period of 16 h or oxidized glutathione for 12 days, and structures were

determined to resolutions ranging from 1.9 to 2.5 Å (Table 1). These experiments delineate the temporal oxidation-dependent conformational changes of RPTPα D2. Exposure of RPTPα D2 to H₂O₂ promotes oxidation of the conserved Cys723 residue of the PTP motif in both molecules of the asymmetric unit. This result confirms original findings that Cys723 is sensitive to oxidation (*41, 42*). We observe formation of the cyclic sulfenamide species in both molecules of RPTPα D2 on incubation with H₂O₂ for 90 min (Figures 2A and 3A); however, their rates of formation and overall stability differ. Prolonged exposure (16 h) to H₂O₂ resulted in conversion of the cyclic sulfenamide to the more oxidized SO₂ species in MolB, although in MolA the cyclic sulfena-mide at the catalytic site remains unchanged relative to a 90 min H₂O₂ incubation (Figures 2B and 3B). Furthermore, whereas incubation of RPTPα D2 crystals for 12 days in 10 mM oxidized glutathione generates the terminally oxidized
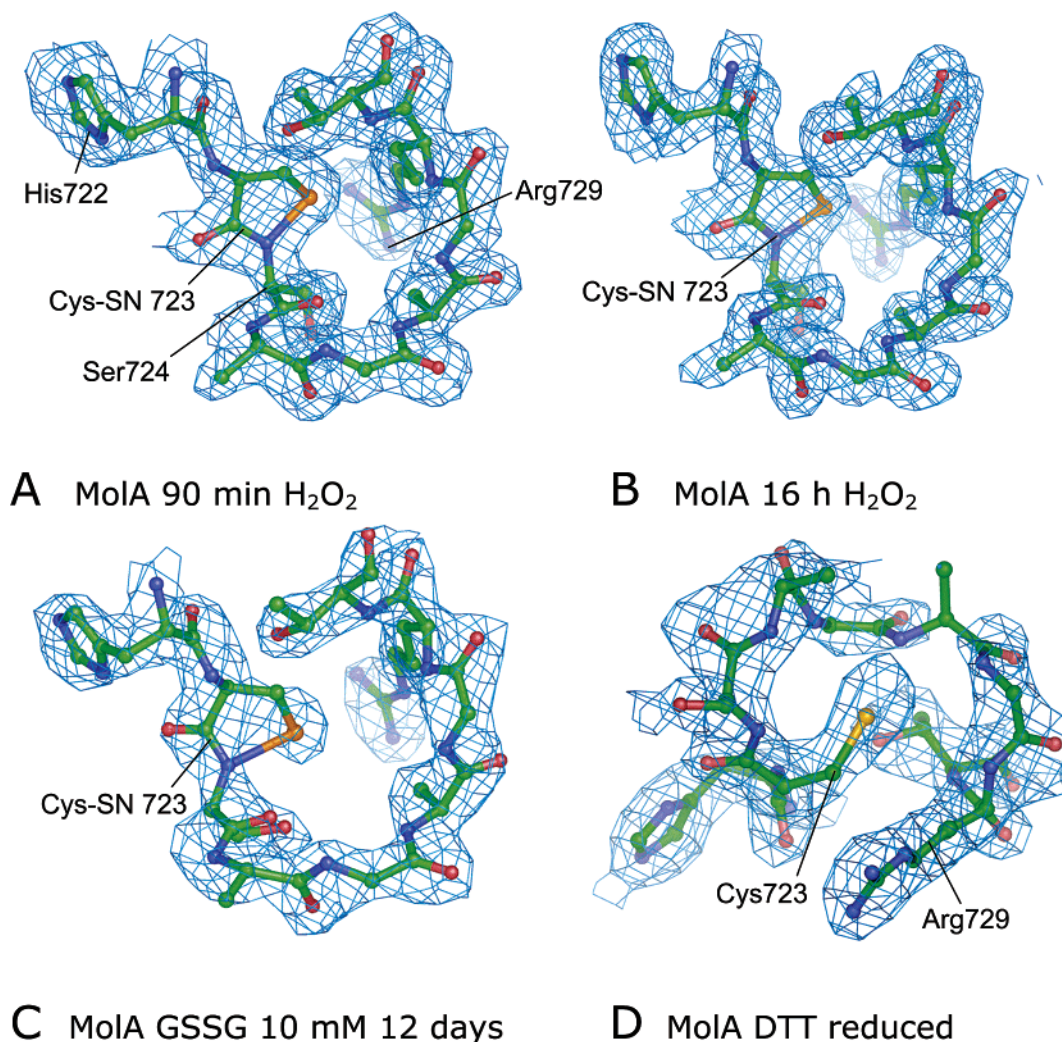
FIGURE 2: Electron density maps of oxidation states of the PTP loop of RPTPα D2 (MolA). Cyclic sulfenamide forms rapidly and is resistant to stronger oxidation. The $2F_o - F_c$ electron density map (contoured at 1σ) of the PTP loop is shown. (A) Cyclic sulfenamide forms after 90 min upon exposure to 50 μM H_2O_2 and is stable (B) for 16 h and (C) on exposure to 10 mM oxidized glutathione for 12 days. (D) Reduction of cyclic sulfenamide with DTT restores the native thiol. Cys-SN 723 denotes the cyclic sulfenamide species.

sulfonic acid (SO_3) derivative of Cys723 in MolB (Figure 3C), a cyclic sulfenamide species is present in MolA (Figure 2C). These findings indicate significant differences in the stability of the cyclic sulfenamide between the two molecules of RPTPα D2 of the asymmetric unit. As discussed below, one explanation for this variation in stability is the difference between the PTP loop conformations in the cyclic sulfenamide states of molecules A and B. As for PTP1B (*18, 19*), in both reduced and oxidized states, the WPD loop adopts the open conformation.

Rates of formation of the cyclic sulfenamide species also differ between the two molecules. Following a 30 min exposure to H_2O_2, electron density corresponding to Cys723 is consistent with a mixture of reduced and oxidized species of the protein. In MolA, this density was modeled using partial occupancy refinement assuming a conversion of ~60% of molecules to the cyclic sulfenamide, with ~40% remaining as the reduced thiol state (Figure 1A of the Supporting Information). As in the oxidation of PTP1B, there was no evidence for a sulfenic acid intermediate, suggesting that sulfenic acid formation is rate-limiting, spontaneously condensing to the cyclic sulfenamide species. Oxidation of Cys723 in MolB is slower, with only ~10−20% of MolB being present as the cyclic sulfenamide at the 30 min time

point (Figure 1B of the Supporting Information). Rates of formation of the cyclic sulfenamide in RPTPα are generally similar to those in PTP1B, where complete conversion of the catalytic site Cys residue occurred within 2 h (*18*).

Oxidation of RPTPα D2 Is Associated with Conformational Changes. In the five-atom heterocyclic ring of the sulfenamide species, the Sγ atom of Cys723 forms a covalent bond to the main chain nitrogen atom of Ser724 and the distance between these two atoms refines to 1.5 Å (Figures 1B and 2A). The conformation of the heterocyclic ring of RPTPα D2 MolA and MolB is identical to the equivalent cyclic sulfenamide of PTP1B (*18, 19*) (Figure 1D). In PTP1B, formation of the cyclic sulfenamide is accompanied by profound conformational changes in the PTP loop and adjacent pTyr recognition loop. The PTP loop converts from a closed helical conformation to an open reverse β-hairpin that exposes the Sγ atom of the cyclic sulfenamide species. Conformational changes of the PTP loop disrupt a hydrogen bond to Tyr46 of the pTyr recognition loop, promoting a displacement of Tyr46 to a solvent-exposed position, accompanied by shifts of the pTyr recognition loop (Figure 1D).

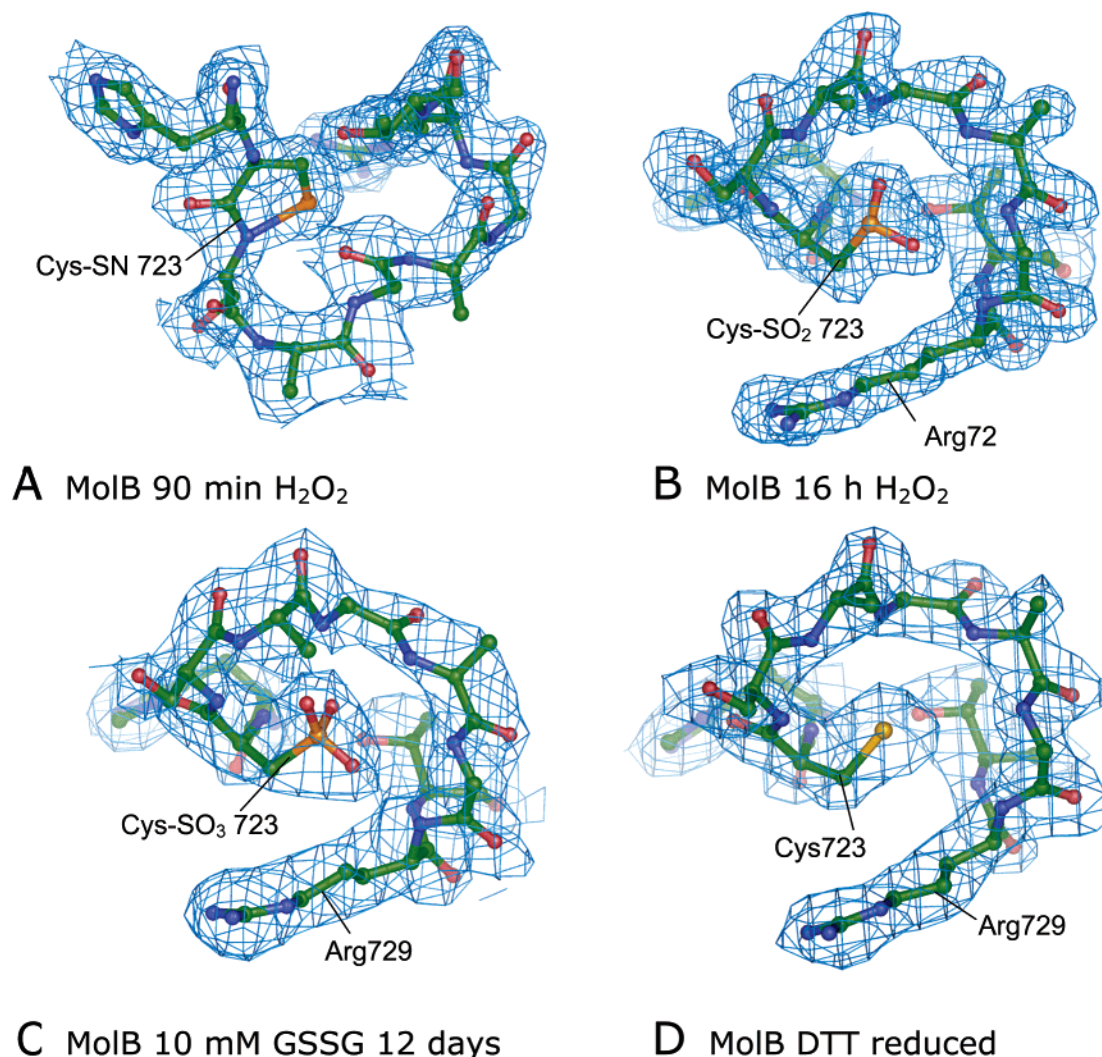In RPTPα D2, the extent of conformational changes produced by oxidation to the cyclic sulfenamide species is

A MolB 90 min H_2O_2

B MolB 16 h H_2O_2

C MolB 10 mM GSSG 12 days

D MolB DTT reduced

FIGURE 3: Electron density maps of oxidation states of the PTP loop of RPTPα D2 (MolB). The $2F_o - F_c$ electron density map (contoured at 1σ) of the PTP loop is shown. Cyclic sulfenamide forms after 90 min upon exposure to 50 μM H_2O_2; (B) by 16 h, cyclic sulfenamide has oxidized to SO_2 and (C) to SO_3 upon exposure to 10 mM oxidized glutathione for 12 days. (D) As in MolA, reduction of cyclic sulfenamide with DTT restores native thiol.

less pronounced than for PTP1B. In both molecules, conformational changes are confined to the PTP loop (Figure 1; Figure 2A of the Supporting Information). In MolA, the PTP loop adopts an open conformation, essentially identical to that in PTP1B, exposing the Sγ atom of the Cys723 cyclic sulfenamide (Figure 1B,D). In RPTPα D2, the PTP and pTyr loops are not connected via a hydrogen bond, and as a consequence, in contrast to PTP1B, motion of the PTP loop is not accompanied by pTyr loop conformational changes. In native, reduced RPTPα D2, the guanidinium group of a buried and invariant Arg residue of the Q-loop (Arg763, equivalent to Arg257 of PTP1B) stabilizes the closed PTP loop via hydrogen bonds with main chain carbonyl groups of PTP loop residues Ala725 and Gly726. In MolA, opening of the PTP loop disrupts these hydrogen bonds and exposes Arg763 to solvent, creating a pocket between Arg763 and the PTP loop. In the crystal, a sulfate anion engages this pocket, accepting hydrogen bonds from the side chain of Arg763 and the main chain amide of Gly726 (Figure 1B).

The oxidized PTP loop of MolB is more similar to the closed reduced conformation than to the open oxidized states of PTP1B and MolA of RPTPα D2. In MolB, only residue

Gly726 changes conformation by (3.6 Å) upon oxidation (Figure 1C; Figure 2A,B of the Supporting Information).

The Cyclic Sulfenamide Species Is Reduced by Thiols. As observed for PTP1B, incubation of oxidized RPTPα D2 crystals with 10 mM DTT for 3 h reduced the cyclic sulfenamide species to the free thiol and restored the conformation of the PTP loop to the native state (Figures 2D and 3D), demonstrating that the cyclic sulfenamide is a reversibly oxidized form of RPTPα D2.

The Cyclic Sulfenamide of RPTPα D2 Is Stable in Solution. Our results revealed differences in oxidation kinetics and conformational changes of the PTP loop between the two RPTPα D2 molecules of the asymmetric unit. Formation of the cyclic sulfenamide occurs earlier in MolA (within 30 min) and is resistant to stronger oxidation for at least 12 days, the maximum time of our incubation (Table 1). In contrast, in MolB, although the cyclic sulfenamide is fully formed after 90 min and remains for 6 h, as for MolA (Figure 1C,D of the Supporting Information), overnight oxidation leads to formation of sulfinic acid that is further oxidized to the sulfonic acid after 12 days (Figure 3B,C). In addition, compared with that in MolA, formation of the cyclic

sulfenamide in MolB is not associated with large conformational changes in the PTP loop (Figure 1C; Figure 2B of the Supporting Information). Differences in the kinetics of cyclic sulfenamide formation and oxidation, and conformational flexibility of the PTP loop, between MolA and MolB presumably reflect differences in their crystallographic environments.

To investigate the stability of the reversibly oxidized state of RPTPα D2 in solution over prolonged exposures to hydrogen peroxide and therefore to determine which molecule of RPTPα D2 of the asymmetric unit correlates better with the stability of the reversibly oxidized form of the phosphatase in solution, we monitored the oxidation of RPTPα D2 by means of the oxPTP antibody that recognizes the triply oxidized (SO_3) state of the catalytic Cys residue (*41*). In the first experiment, we monitored the formation of the reversibly oxidized state in 0.1 mM H_2O_2 over a 24 h time period using the procedure of Persson et al. (*41*) (sequential steps of oxidation, alkylation, reduction, and pervanadate oxidation) [Figure 4B, scheme I (ARP)]. Oxidation is maximal within 2 h of treatment and remains constant for 24 h (Figure 4A, left panel). We routinely observe a doublet upon processing of RPTPα D2, even in the RPTPα D2 C723S mutant (data not shown), indicating that doublet formation is not linked to the catalytic Cys723. However, this experiment does not distinguish between reversibly, doubly, and triply oxidized forms of the protein since all oxidized states of the catalytic Cys will convert to SO_3 on pervanadate incubation [Figure 4B, scheme I (ARP)]. To investigate the amount of triply oxidized RPTPα D2 (Cys-SO_3) following H_2O_2 incubation, the oxidized protein was directly blotted by the oxPTP antibody, omitting the alkylation, reduction, and pervanadate oxidation treatments. Figure 4A (right panel) indicates that very little RPTPα D2 is oxidized to the triply oxidized state even after being exposed to 0.1 mM H_2O_2 for 24 h. To test for doubly oxidized RPTPα D2 (Cys-SO_2), which is not directly recognized by the oxPTP antibody, a variation of the method of Persson et al. (*41*) was employed [Figure 4B, scheme II (RAP)]. In this experiment, the protein was first treated with 1 mM H_2O_2 for 30 min and then incubated with DTT to reduce reversibly oxidized cysteines (SOH, disulfides, and sulfenamides) to free thiols. Next, free thiols were alkylated, and sulfinic acid-modified cysteines were oxidized to sulfonic acid using pervanadate. The triply oxidized cysteines were then detected using the oxPTP antibody. Only very low levels of doubly oxidized RPTPα D2 are formed (Figure 5A, RAP lane), since the amount of triply oxidized RPTPα D2 following this procedure is only slightly greater than that produced following exposure to H_2O_2 alone (Figure 5A, NP lane), consistent with MALDI-ToF data we obtained previously (*42*). Finally, we investigated reversible, double, and triple oxidation of RPTPα D2 in response to 0.1 mM H_2O_2 over time and found only trace amounts of double and triple oxidation of RPTPα D2 (Figure 5B).

The time-dependent generation of oxidized species of RPTPα D2 in the presence of H_2O_2 was also monitored using MALDI-ToF mass spectrometry (Figure 6). In this experiment, the protein was incubated in H_2O_2, alkylated, and then reduced (Figure 4B, scheme III). Following this procedure, reversibly oxidized cysteines will exist as reduced cysteines, whereas nonoxidized cysteines will be alkylated. As a
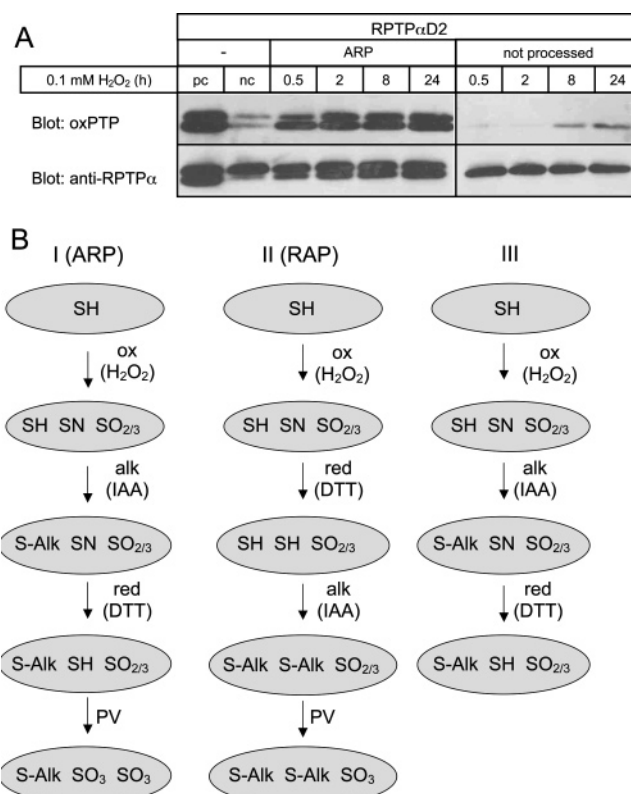

FIGURE 4: Stable reversible oxidation of RPTPα D2. (A) RPTPα D2 was treated with 0.1 mM H_2O_2 for different periods of time as indicated and processed for detection of reversible oxidation using the oxPTP antibody as described in Experimental Procedures. The samples were run on a SDS−PAGE gel and blotted. The immunoblots were probed with the oxPTP antibody (top) and subsequently with the anti-RPTPα antibody to monitor equal loading of protein. The immunoblots were developed with enhanced chemiluminescence (ECL). The samples were processed for detection using the oxPTP antibody by alkylation, reduction, and pervanadate treatment for detection of reversible oxidation (ARP), or the samples were loaded directly on a SDS−PAGE gel for detection of irreversible triple oxidation (not processed). For the positive control (pc), the sample is treated as described for panel B [scheme I (ARP)] without steps 1 (ox) and 2 (alk). The sample is treated with DTT (red) and subsequently with pervanadate (PV), leading to maximal sulfonic acid formation. For the negative control (nc), the sample is treated as described for panel B [scheme I (ARP)], but instead of H_2O_2 treatment in the first step, the sample is treated with 10 mM DTT for 20 min and subsequently processed (alk, red, PV), leading to maximal alkylation and minimal sulfonic acid formation. (B) Schematic of oxidation, reduction, and alkylation schemes for detection of reversibly oxidized species of RPTPα D2 in solution using the oxPTP antibody and mass spectrometry mentioned in the text and Figures 4A and 5.

positive control, RPTPα D2 was treated with pervanadate, resulting in double and triple oxidation. Figure 6 shows that during the 24 h time course of H_2O_2 treatment the proportion of reduced to alkylated cysteine increases, whereas the amount of sulfinic and sulfonic acid remains very small, demonstrating that time-dependent reversible oxidation of Cys723 is stable.

Catalytic Activity Measurements. RPTPα D2 has some 50-fold lower catalytic activity than the D1 domain, with a low affinity for *p*NPP (K_m = 21 mM) (*38*). However, by measuring the catalytic activity of RPTPα D2 using 50 mM *p*NPP, we determined the proportion of the protein that was reversibly oxidized upon prolonged exposure to 50 μM H_2O_2. Incubation of RPTPα D2 with H_2O_2 for 18 h at 14 °C
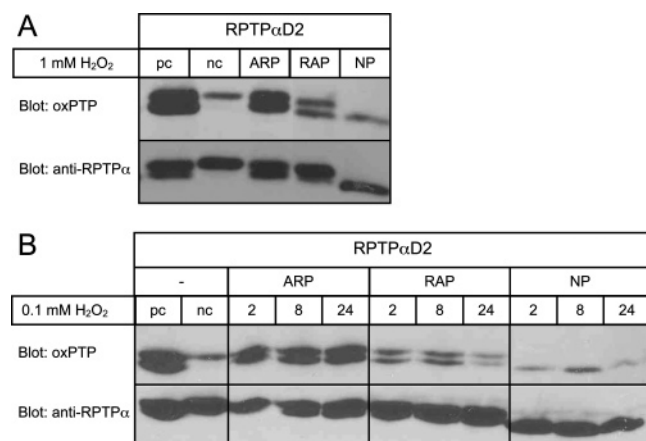
FIGURE 5: Irreversible oxidation of RPTPα D2 is limited. (A) RPTPα D2 was treated with 1 mM H₂O₂ for 0.5 h and processed for detection of reversible oxidation: alkylation, reduction, and pervanadate treatment (ARP), processed for detection of irreversible oxidation, or reduction, alkylation, and pervanadate treatment (RAP), or not processed for detection of direct triple oxidation (NP). (B) Like panel A except 0.1 mM H₂O₂ was used for prolonged periods of time as indicated. ARP and RAP defined in the text and the legend of Figure 4B.
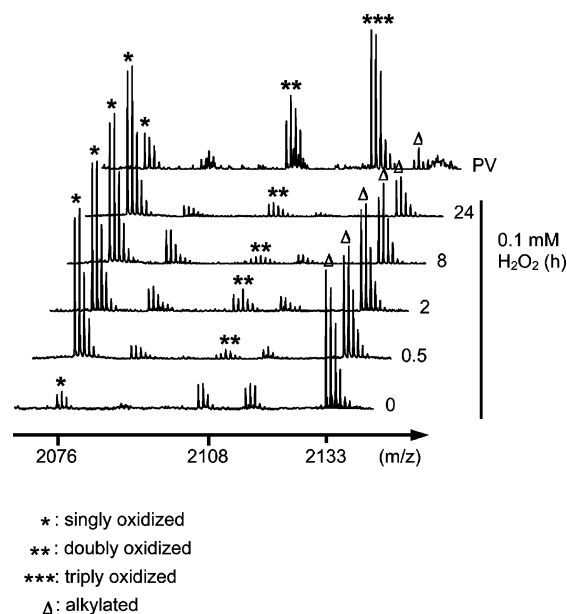

★: singly oxidized
★★: doubly oxidized
★★★: triply oxidized
Δ: alkylated

FIGURE 6: Reversibly oxidized RPTPα D2 is stable. Purified RPTPα D2 was treated with 0.1 mM H₂O₂ for different periods of time (from 0 to 24 h) or as a control for irreversible oxidation with 1 mM pervanadate (PV) for 30 min. To protect the samples after H₂O₂ and PV treatment against further oxidation during the protease digestions, the reduced cysteines were alkylated using iodoacetamide and the reversibly oxidized cysteines were reduced using DTT. Subsequently, the samples were kept under reducing conditions. MALDI-ToF spectra were acquired as described in Experimental Procedures. The m/z range that contains the active site Cys723 peptide (residues 710−729) is depicted. The reversibly oxidized Cys723 peptide was detected in reduced form (m/z 2075.98, one asterisk); the sulfinic acid-containing peptide shifted +32.00 to m/z 2107.98 (two asterisks), and the sulfonic acid-containing peptide shifted +48.00 to m/z 2123.98 (three asterisks). The reduced Cys723-containing peptide was detected in alkylated form with a shift in relative molecular mass of +57.02 (m/z 2133.00, Δ).

completely inactivated the enzyme. Exposure of the oxidized protein to 25 mM DTT for 3 h restored the specific activity to 72.5% (mean of two experiments, range from 72.4 to 72.5%) of its pre-oxidation activity. In control experiments

in the presence of 5 mM DTT, no loss of phosphatase activity was observed after 21 h. These results indicate that the majority of RPTPα D2 exists as a reversibly oxidized state on prolonged exposure to H₂O₂. Failure to recover all catalytic activity on reduction with DTT suggested that a small proportion of the protein was irreversibly oxidized, most likely modified to the higher oxidized sulfinic and sulfonic states, in agreement with the Western blot studies showing small amounts of these species on exposure to 100 μM H₂O₂ for 24 h (Figures 4A and 5B).

Together, these results demonstrate that in solution, the majority of RPTPα D2 (~72%) exists in the reversibly oxidized state on prolonged exposure to H₂O₂ (18−24 h) and is therefore resistant to stronger oxidation. This correlates better with the stability of the cyclic sulfenamide observed in MolA of the crystal structure. Whereas in MolA, electron density consistent with the cyclic sulfenamide is observed on 16 h exposure to H₂O₂, in MolB Cys723 was oxidized to sulfinic acid (Figures 2B and 3B).

RPTPα D2 Is a Monomer in Solution. Using calibrated gel filtration chromatography, we determined the apparent molecular mass of RPTPα D2 to be 28 kDa (calculated mass of 31 kDa) (data not shown), consistent with a monomeric state of the protein in solution. Our findings confirm those of Sonnenburg et al., who determined that RPTPα D2, as well as the RPTPα D1D2 protein, is a monomer in solution as assessed by gel filtration and dynamic light scattering (*35*). The apparent molecular mass of RPTPα D2 did not change on conversion to the oxidized state, indicating that oxidation of the phosphatase did not promote protein dimerization. The dimers of RPTPα D2 we observe in the crystal, similar to that of Sonnenburg et al. (*35*) and favored by the crystallization conditions, may contribute to the interaction interface within constitutive RPTPα dimers observed within a cellular context (*51*, *52*). However, additional factors, such as the involvement of other domains of RPTPα and/or the membrane environment, are likely to stabilize RPTPα dimers in vivo.

DISCUSSION

The Cyclic Sulfenamide as a Universal Feature of Reversibly Oxidized Conventional PTPs. In this study, we demonstrate that RPTPα D2 is reversibly oxidized via a cyclic sulfenamide species. The cyclic sulfenamide is promoted by oxidants H₂O₂ and oxidized glutathione and reduced by DTT. The discovery of the cyclic sulfenamide in RPTPα D2 is only the second example of such a species in any protein and the first report of a RPTP D2. However, the existence of a cyclic sulfenamide in two distinct PTP domains suggests that its formation is not unique to PTP1B (*18*, *19*) but will likely be a general feature of catalytic Cys oxidation in conventional PTPs. Oxidation of DSPs, lmPTPs, Cdc25, and lipid phosphatases that feature cysteine residues in the proximity of the catalytic Cys promotes disulfide bond formation (*5*). Interestingly, only one conventional PTP, mPEP, shares a proximal Cys equivalent to those of KAP and PTEN (*33*), and it will be interesting to determine whether a cyclic sulfenamide or disulfide bond represents the reversibly oxidized state of this protein.

The role of the catalytic Cys of RPTP D2s as a redox sensor may explain their conservation in domains with little

or no phosphatase catalytic activity (*4*). Structural features of the phosphatase catalytic site are conserved in D2s to create the microenvironment necessary for the reduced pK_a of the catalytic Cys residue essential for its role as a redox sensor. These include a positive electrostatic potential created by the conserved Arg residues of the PTP motif and the Q-loop (Arg729 and Arg763, respectively), the hydrogen bond between side chains of Cys723 and Thr730 of the PTP loop, and the orientation of the main chain amides of the PTP loop toward the thiol of Cys723 (Figure 1B). Kinetic data indicate that the Arg residue of the PTP C(X)$_5$R motif together with a histidine residue immediately N-terminal to the PTP motif, conserved in PTPs, contributes to the reduced pK_a of the catalytic Cys residue (*16*, *53*). Interestingly, the PTP signature motif of conventional tyrosine specific PTPs comprises three highly conserved glycine residues: Cys-Ser-Xaa-Gly-Xaa-Gly-Arg-(Ser/Thr)-Gly. The conformational flexibility conferred by glycines may permit opening of the PTP loop and stabilization of the cyclic sulfenamide. Both the PTP loops of PTP1B and RPTPα D2 MolA adopt the same open conformation upon formation of the cyclic sulfenamide, and in RPTPα D2, this is associated with its resistance to stronger oxidation observed in the crystal.

Implications for Oxidation-Dependent RPTPα Conformational Changes and Regulation. A mechanism for regulating RPTP catalytic activity involving formation of inhibitory RPTP dimers, proposed on the basis of the crystal structure of RPTPα D1 dimers, in which wedge elements of each subunit insert into the catalytic site of the opposing monomer (*48*), is consistent with a range of biochemical and cellular studies (*54*−*56*). Significantly, the structure explained earlier observations that signaling from a chimera of the extracellular and transmembrane regions of EGFR fused to the cytosolic domain of CD45 was negatively regulated by EGF-induced dimerization (*54*). However, crystal structures of the LAR and CD45 tandem D1 and D2 domains showed that formation of the inhibitory D1 interface would be prevented by a steric clash between the D2 domains of the dimer, which could be relieved only by conformational changes which alter the D1−D2 domain interface (*34*, *50*). The relative orientation of the LAR and CD45 D1 and D2 domains is similar, constrained by a short four-residue linker, and stabilized by a set of extensive interactions (Figure 7A). LAR and CD45 residues that mediate interdomain contacts, together with the linker region, are highly conserved in RPTPα (*34*), suggesting that the relative orientation of D1 and D2 in RPTPα will be similar to that in LAR and CD45 (Figure 7).

Substantial evidence now indicates that oxidation of Cys723 of RPTPα causes changes in RPTPα tertiary and quaternary structures. Oxidation induces changes in FRET between GFP derivatives attached to the N-terminus of α1′ and the C-terminal α-helix of RPTPα D2 (α6, Figure 7A) (*39*) and alters the protein's sensitivity to trypsinolysis (A. Groen, J. Overvoorde, L. Tertoolen, T. van der Wijk, and J. den Hertog, unpublished observations). These tertiary structural changes are associated with changes in quaternary structure in such a way that preexisting RPTPα dimers are stabilized and their rotational coupling is induced (*39*, *40*).

In RPTPα D2 crystals, oxidation-dependent conformational changes are confined to the PTP loop. Unlike that in PTP1B, the neighboring pTyr loop is not altered, and therefore, conformational changes of the PTP loop are not
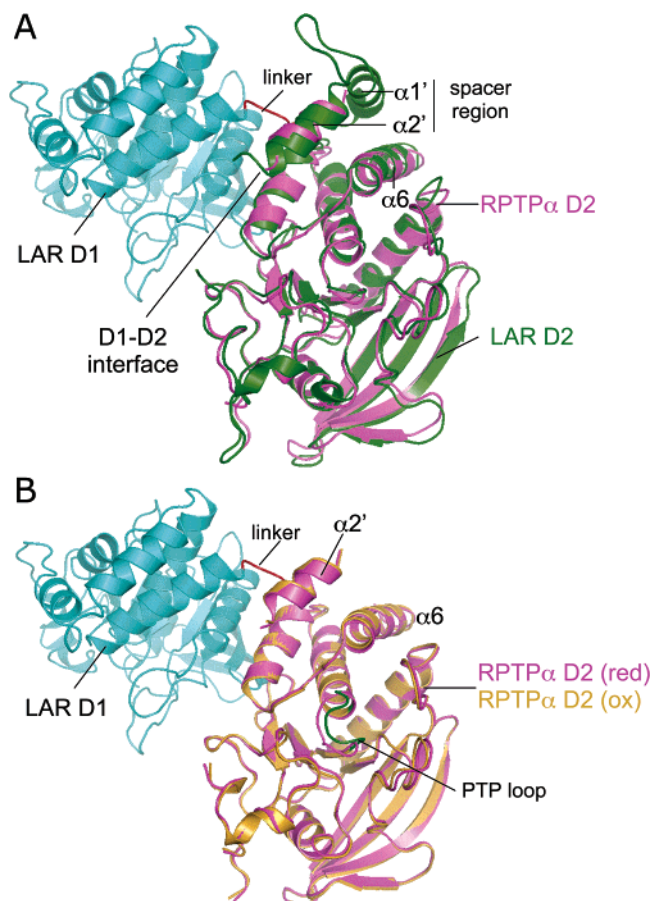

FIGURE 7: Consequences of RPTPα D2 oxidation for the D1−D2 interface. Superimposition of RPTPα D2 (reduced and oxidized) onto D2 of LAR. (A) D2 of RPTPα (purple) superimposed onto D2 (green) of LAR. The linker region of LAR is colored red, and LAR D1 is colored blue. (B) Oxidized and reduced RPTPα D2 (MolA) relative to D1 of LAR. LAR D2 has been omitted for clarity. Oxidation-induced conformational changes of the RPTPα D2 catalytic site do not directly alter the D1−D2 interdomain interface.

directly transmitted to residues of RPTPα D2 that, on the basis of sequence conservation with LAR and CD45, would be predicted to participate at the D1−D2 domain interface (Figure 7B). The more extensive oxidation-dependent conformational changes of RPTPα D2 required an explanation of oxidation-dependent suppression of RPTPα activity, and coupled tertiary and quaternary conformational changes that are not observed in our crystallographic study. One possible explanation is that crystal lattice contacts limit the capacity of RPTPα D2 to undergo conformational change in response to oxidation. Our finding that the two molecules of RPTPα D2 respond differently to H_2O_2 supports the notion that lattice contacts influence the extent of conformational change. Furthermore, our efforts to crystallize oxidized RPTPα D2 were unsuccessful, a result which could be explained if the oxidized protein adopted a conformation different from those observed in the crystal. It is also possible that the absence of the putative α1′ helix in our RPTPα D2 crystals could prevent large conformational changes if α1′ were required to stabilize the oxidized conformation of RPTPα D2. Alternatively, an allosteric mechanism could be invoked to explain how oxidation of Cys723 promotes changes at the D1−D2 interface. In this model, more extensive RPTPα tertiary and quaternary conformational changes promoted by

Cys723 oxidation occur only in the context of the entire RPTPα protein. The RPTPα extracellular and transmembrane domains are independently capable of homodimerization (*51*, *52*), whereas RPTPα D2 homodimerizes upon Cys723 oxidation (*39*). Oxidation of Cys723 (presumably by causing conformational changes of the PTP loop altering the protein's molecular surface) promotes D2−D2 associations (*39*) affecting the overall quaternary structure of RPTPα. The oxidation-induced association of D2 domains could be triggered by changes in the surface properties of D2 resulting from generation of the cyclic sulfenamide and opening of the PTP loop or, as suggested by van der Wijk et al. (*57*), be mediated by intermolecular disulfides involving Cys723.

In conclusion, our data demonstrate that oxidation of Cys723 of RPTPα D2 yields a reversible cyclic sulfenamide species, associated with conformational changes in the PTP loop. However, these limited structural changes are insufficient for explaining H_2O_2-mediated dimerization, and more extensive tertiary conformational changes within RPTPα D2 may be expected in the context of the full-length RPTPα protein, and without the constraints imposed by the crystal lattice.

ACKNOWLEDGMENT

SUPPORTING INFORMATION AVAILABLE

Electron density maps of various oxidation states of the PTP loop of RPTPα D2 (Figure 1) and oxidation-induced structural changes in RPTPα D2 (Figure 2). This material is available free of charge via the Internet at http://pubs.acs.org.

REFERENCES

1. Alonso, A., Sasin, J., Bottini, N., Friedberg, I., Friedberg, I., Osterman, A., Godzik, A., Hunter, T., Dixon, J., and Mustelin, T. (2004) Protein tyrosine phosphatases in the human genome, *Cell 117*, 699−711.
2. Finkel, T. (2003) Oxidant signals and oxidative stress, *Curr. Opin. Cell Biol. 15*, 247−254.
3. Rhee, S. G., Bae, Y. S., Lee, S.-R., and Kwon, J. (2000) Hydrogen peroxide: A key messenger that modulates protein phosphorylation through cysteine oxidation, *Sci. STKE P1*, 2000.
4. den Hertog, J., Groen, A., and van der Wijk, T. (2005) Redox regulation of protein-tyrosine phosphatases, *Arch. Biochem. Biophys. 434*, 11−15.
5. Salmeen, A., and Barford, D. (2005) Functions and mechanisms of redox regulation of cysteine-based phosphatases, *Antioxid. Redox Signaling 7*, 560−577.
6. Tonks, N. K. (2005) Redox redux: Revisiting PTPs and the control of cell signaling, *Cell 121*, 667−770.
7. Bae, Y. S., Kang, S. W., Seo, M. S., Baines, I. C., Tekle, E., Chock, P. B., and Rhee, S. G. (1997) Epidermal Growth Factor (EGF)-induced Generation of Hydrogen Peroxide, *J. Biol. Chem. 272*, 217−221.
8. Sundaresan, M., Yu, Z. X., Ferrans, V. J., Irani, K., and Finkel, T. (1995) Requirement for generation of H_2O_2 for platelet-derived growth factor signal transduction, *Science 270*, 296−299.
9. Knebel, A., Rahmsdorf, H. J., Ullrich, A., and Herrlich, P. (1996) Dephosphorylation of receptor tyrosine kinases as target of regulation by radiation, oxidants or alkylating agents, *EMBO J. 15*, 5314−5325.
10. Lee, S. R., Kwon, K. S., Kim, S. R., and Rhee, S. G. (1998) Reversible inactivation of protein-tyrosine phosphatase 1B in A431 cells stimulated with epidermal growth factor, *J. Biol. Chem. 273*, 15366−15372.
11. Mahadev, K., Zilbering, A., Zhu, L., and Goldstein, B. J. (2001) Insulin-stimulated hydrogen peroxide reversibly inhibits protein-tyrosine phosphatase 1B in vivo and enhances the early insulin action cascade, *J. Biol. Chem. 276*, 21938−21942.
12. Guan, K. L., and Dixon, J. E. (1991) Evidence for protein-tyrosine-phosphatase catalysis proceeding via a cysteine-phosphate intermediate, *J. Biol. Chem. 266*, 17026−17030.
13. Denu, J. M., Lohse, D. L., Vijayalakshmi, J., Saper, M. A., and Dixon, J. E. (1996) Visualization of intermediate and transition-state structures in protein-tyrosine phosphatase catalysis, *Proc. Natl. Acad. Sci. U.S.A. 93*, 2493−2498.
14. Denu, J. M., and Dixon, J. E. (1998) Protein tyrosine phosphatases: Mechanisms of catalysis and regulation, *Curr. Opin. Chem. Biol. 2*, 633−641.
15. Pannifer, A. D., Flint, A. J., Tonks, N. K., and Barford, D. (1998) Visualization of the cysteinyl-phosphate intermediate of a protein-tyrosine phosphatase by X-ray crystallography, *J. Biol. Chem. 273*, 10454−10462.
16. Zhang, Z. Y., and Dixon, J. E. (1993) Active site labeling of the *Yersinia* protein tyrosine phosphatase: The determination of the pK_a of the active site cysteine and the function of the conserved histidine 402, *Biochemistry 32*, 9340−9345.
17. Denu, J. M., and Tanner, K. G. (1998) Specific and reversible inactivation of protein tyrosine phosphatases by hydrogen peroxide: Evidence for a sulfenic acid intermediate and implications for redox regulation, *Biochemistry 37*, 5633−5642.
18. Salmeen, A., Andersen, J. N., Myers, M. P., Meng, T. C., Hinks, J. A., Tonks, N. K., and Barford, D. (2003) Redox regulation of protein tyrosine phosphatase 1B involves a sulfenyl-amide intermediate, *Nature 423*, 769−773.
19. van Montfort, R. L., Congreve, M., Tisi, D., Carr, R., and Jhoti, H. (2003) Oxidation state of the active-site cysteine in protein tyrosine phosphatase 1B, *Nature 423*, 773−777.
20. Song, H., Hanlon, N., Brown, N. R., Noble, M. E., Johnson, L. N., and Barford, D. (2001) Phosphoprotein-protein interactions revealed by the crystal structure of kinase-associated phosphatase in complex with phospho-CDK2, *Mol. Cell 7*, 615−626.
21. Fauman, E. B., Cogswell, J. P., Lovejoy, B., Rocque, W. J., Holmes, W., Montana, V. G., Piwnica-Worms, H., Rink, M. J., and Saper, M. A. (1998) Crystal structure of the catalytic domain of the human cell cycle control phosphatase, Cdc25A, *Cell 93*, 617−625.
22. Sohn, J., and Rudolph, J. (2003) Catalytic and chemical competence of regulation of cdc25 phosphatase by oxidation/reduction, *Biochemistry 42*, 10060−10070.
23. Buhrman, G., Parker, B., Sohn, J., Rudolph, J., and Mattos, C. (2005) Structural mechanism of oxidative regulation of the phosphatase Cdc25B via an intramolecular disulfide bond, *Biochemistry 44*, 5307−5316.
24. Chirarugi, P., Fiaschi, T., Taddei, M. L., Talini, D., Giannoni, E., Raugei, G., and Ramponi, G. (2001) Two vicinal cysteines confer a peculiar redox regulation to low molecular weight protein tyrosine phosphatase in response to patelet-derived growth factor receptor timulation, *J. Biol. Chem. 276*, 33478−33487.
25. Leslie, N. R., Bennett, D., Lindsay, Y. E., Stewart, H., Gray, A., and Downes, C. P. (2003) Redox regulation of PI 3-kinase signalling via inactivation of PTEN, *EMBO J. 22*, 5501−5510.
26. Morin, R. B., Gordon, E. M., and Lake, J. R. (1973) Chemistry of dehydropeptides. Formation of isothiazolones and isothiazolidones from cysteine peptides, *Tetrahedron Lett. 52*, 5213−5216.
27. Morin, R. B., and Gordon, E. M. (1973) Chemistry of dehydropeptides. A rearrangement of an isothiazolone, *Tetrahedron Lett.*, 2159−2162.
28. Kim, W., Dannaldson, J., and Gates, K. S. (1996) Reactions of 3H-1,2-benzodithiol-3-one 1-oxide with amines and anilines, *Tetrahedron Lett. 37*, 5337−5340.
29. Sivaramakrishnan, S., Keerthi, K., and Gates, K. S. (2005) Chemical Model for Redox Regulation of Protein Tyrosine Phosphatase1B (PTP1B) Activity, *J. Am. Chem. Soc. 127*, 10830−10831.
30. Meng, T. C., Fukada, T., and Tonks, N. K. (2002) Reversible oxidation and inactivation of protein tyrosine phosphatases in vivo, *Mol. Cell 9*, 387−399.
31. Mahadev, K., Wu, X., Zilbering, A., Zhu, L., Lawrence, J. T., and Goldstein, B. J. (2001) Hydrogen peroxide generated during cellular insulin stimulation is integral to activation of the distal

insulin signaling cascade in 3T3-L1 adipocytes, *J. Biol. Chem. 276*, 48662−48669.

32. Meng, T. C., Buckley, D. A., Galic, S., Tiganis, T., and Tonks, N. K. (2004) Regulation of insulin signaling through reversible oxidation of the protein-tyrosine phosphatases TC45 and PTP1B, *J. Biol. Chem. 279*, 37716−37725.

33. Andersen, J. N., Jansen, P. G., Echwald, S. M., Mortensen, O. H., Fukada, T., Del Vecchio, R., Tonks, N. K., and Moller, N. P. (2004) A genomic perspective on protein tyrosine phosphatases: Gene structure, pseudogenes, and genetic disease linkage, *FASEB J. 18*, 8−30.

34. Nam, H. J., Poy, F., Krueger, N. X., Saito, H., and Frederick, C. A. (1999) Crystal structure of the tandem phosphatase domains of RPTP LAR, *Cell 97*, 449−457.

35. Sonnenburg, E. D., Bilwes, A., Hunter, T., and Noel, J. P. (2003) The structure of the membrane distal phosphatase domain of RPTPα reveals interdomain flexibility and an SH2 domain interaction region, *Biochemistry 42*, 7904−7914.

36. Jia, Z., Barford, D., Flint, A. J., and Tonks, N. K. (1995) Structural basis for phosphotyrosine peptide recognition by protein tyrosine phosphatase 1B, *Science 268*, 1754−1758.

37. Lim, K. L., Kolatkar, P. R., Ng, K. P., Ng, C. H., and Pallen, C. J. (1998) Interconversion of the kinetic identities of the tandem catalytic domains of receptor-like protein-tyrosine phosphatase PTPα by two point mutations is synergistic and substrate-dependent, *J. Biol. Chem. 273*, 28986−28993.

38. Buist, A., Zhang, Y. L., Keng, Y. F., Wu, L., Zhang, Z. Y., and den Hertog, J. (1999) Restoration of potent protein-tyrosine phosphatase activity into the membrane-distal domain of receptor protein-tyrosine phosphatase α, *Biochemistry 38*, 914−922.

39. Blanchetot, C., Tertoolen, L. G., and den Hertog, J. (2002) Regulation of receptor protein-tyrosine phosphatase α by oxidative stress, *EMBO J. 21*, 493−503.

40. van der Wijk, T., Blanchetot, C., Overvoorde, J., and den Hertog, J. (2003) Redox-regulated rotational coupling of receptor protein-tyrosine phosphatase α dimers, *J. Biol. Chem. 278*, 13968−13974.

41. Persson, C., Sjoblom, T., Groen, A., Kappert, K., Engstrom, U., Hellman, U., Heldin, C. H., den Hertog, J., and Ostman, A. (2004) Preferential oxidation of the second phosphatase domain of receptor-like PTPα revealed by an antibody against oxidized protein tyrosine phosphatases, *Proc. Natl. Acad. Sci. U.S.A. 101*, 1886−1891.

42. Groen, A., Lemeer, S., van der Wijk, T., Overvoorde, J., Heck, A. J., Ostman, A., Barford, D., Slijper, M., and den Hertog, J. (2005) Differential oxidation of protein-tyrosine phosphatases, *J. Biol. Chem. 280*, 10298−10304.

43. CCP4 (1994) The CCP4 suite: Programs for protein crystallography, *Acta Crystallogr. D50*, 760−763.

44. Persson, C., Kappert, K., Engstrom, U., Ostman, A., and Sjoblom, T. (2005) An antibody-based method for monitoring in vivo oxidation of protein tyrosine phosphatases, *Methods 35*, 37−43.

45. den Hertog, J., Tracy, S., and Hunter, T. (1994) Phosphorylation of receptor protein-tyrosine phosphatase α on Tyr789, a binding site for the SH3-SH2-SH3 adaptor protein GRB-2 in vivo, *EMBO J. 13*, 3020−3032.

46. Barford, D., Flint, A. J., and Tonks, N. K. (1994) Crystal structure of human protein tyrosine phosphatase 1B, *Science 263*, 1397−1404.

47. Hof, P., Pluskey, S., Dhe-Paganon, S., Eck, M. J., and Shoelson, S. E. (1998) Crystal structure of the tyrosine phosphatase SHP-2, *Cell 92*, 441−450.

48. Bilwes, A. M., den Hertog, J., Hunter, T., and Noel, J. P. (1996) Structural basis for inhibition of receptor protein-tyrosine phosphatase-α by dimerization, *Nature 382*, 555−559.

49. Hoffmann, K. M., Tonks, N. K., and Barford, D. (1997) The crystal structure of domain 1 of receptor protein-tyrosine phosphatase μ, *J. Biol. Chem. 272*, 27505−27508.

50. Nam, H. J., Poy, F., Saito, H., and Frederick, C. A. (2005) Structural basis for the function and regulation of the receptor protein tyrosine phosphatase CD45, *J. Exp. Med. 201*, 441−452.

51. Jiang, G., den Hertog, J., and Hunter, T. (2000) Receptor-like protein tyrosine phosphatase a homodimerizes on the cell surface, *Mol. Cell. Biol. 20*, 5917−5929.

52. Tertoolen, L. G., Blanchetot, C., Jiang, G., Overvoorde, J., Gadella, T. W., Jr., Hunter, T., and den Hertog, J. (2001) Dimerization of receptor protein-tyrosine phosphatase α in living cells, *BMC Cell Biol. 2*, 8.

53. Zhang, Z. Y., Wang, Y., Wu, L., Fauman, E. B., Stuckey, J. A., Schubert, H. L., Saper, M. A., and Dixon, J. E. (1994) The Cys-(X)$_5$Arg catalytic motif in phosphoester hydrolysis, *Biochemistry 33*, 15266−15270.

54. Desai, D. M., Sap, J., Schlessinger, J., and Weiss, A. (1993) Ligand-mediated negative regulation of a chimeric transmembrane receptor tyrosine phosphatase, *Cell 73*, 541−554.

55. Majeti, R., Bilwes, A. M., Noel, J. P., Hunter, T., and Weiss, A. (1998) Dimerization-induced inhibition of receptor protein tyrosine phosphatase function through an inhibitory wedge, *Science 279*, 88−91.

56. Jiang, G., den Hertog, J., Su, J., Noel, J., Sap, J., and Hunter, T. (1999) Dimerization inhibits the activity of receptor-like protein-tyrosine phosphatase α, *Nature 401*, 606−610.

57. van der Wijk, T., Overvoorde, J., and den Hertog, J. (2004) H$_2$O$_2$ induced intermolecular disulfide bond formation between receptor protein-tyrosine phosphatases, *J. Biol. Chem. 279*, 44355−44361.